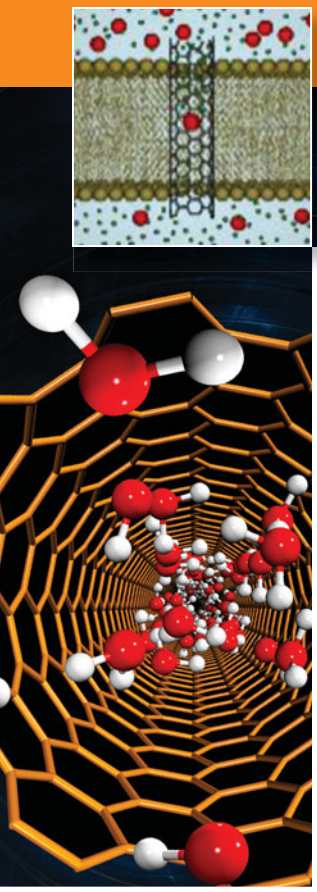


Experimental measurements in single-nanotube fluidic channels

Hyegi Min, Yun-Tae Kim, and Chang Young Lee

Technologies for detecting and analyzing a single molecule help us understand and engineer numerous phenomena observed in nature. Carbon nanotubes (CNTs) are highly efficient molecular conduits due to their atomically smooth surface. Because of their small diameters, comparable to the size of a single molecule, even a single blocking molecule can obstruct CNT fluidic channels. Analyzing these pore-blocking events in CNTs therefore enables single-molecule studies. The high-aspect ratios of CNT channels, which extend the time scale of transport, allow for studying molecular transport that is too fast to record in other systems. Both theoretical studies and ensemble experimental measurements have verified the enhanced flow of various ions and molecular species in CNTs. Experimental measurements of a single-CNT fluidic channel, however, have only recently begun, demonstrating the detection of individual DNA, polymer, and alkali-metal ions. This article reviews recent advances in single-nanotube fluidic channels with a focus on experimental measurements.

Introduction

Carbon nanotubes (CNTs) are well suited for nanofluidic channels[1–3] owing to their remarkable structural features, including nanoscale diameter, high-aspect ratio, and structural uniformity. The graphitic inner wall of a CNT provides atomic smoothness and hydrophobicity that contribute to a nonzero velocity along the wall. Molecules passing through a CNT can attain average velocities that are orders of magnitude higher than the values estimated by the Hagen–Poiseuille Law, making the experimental measurement of flux possible even for a single CNT.

A unique feature of CNT-based nanofluidic channels is that unlike protein-ion channels, which close and open via conformational changes, CNT channels maintain a structurally open state, so the role of a blocking species is crucial when characterizing molecular transport. The blockers tested thus far are molecular species with sizes comparable to the diameter of CNTs, including dyes,[4] DNA,[5,6] nanoparticles,[7] and hydrated ions.[8,9] Recent advances in CNT research allow us to control or measure the diameter, length, and pore properties of CNTs, hence CNT fluidic channels have great potential for single-molecule studies, which have been challenging to conduct reliably using other nanofluidic systems.

Several studies have addressed molecular transport through the small diameter of a CNT channel, proposing applications in desalination of seawater,[10] molecular filtering, drug delivery,[11] and nanoscale reactions.[12] Most of the systems studied were composed of large numbers of CNTs that leave ambiguities in understanding the molecular transport. Single-CNT channels enable the study of single-molecule transport through CNTs with known diameters, lengths, and electrical properties, and thus have become promising platforms for further nanofluidics studies. The design and fabrication of a reliable platform for experimental measurements of a single-CNT channel, however, remains challenging, owing to the small dimensions of these systems.

In this article, we first introduce single-CNT platforms for experimentally measuring transport of various species along the interior of a CNT, including hydrated ions, DNA, and nanoparticles. We then discuss stochastic pore-blocking events from single-CNT channels and the information that can be extracted from the events. We also describe optical detection of molecular translocation through the nanochannel. Finally, we discuss future research directions of nanopore studies and the challenges to overcome.

Experimental platforms for studying single-nanotube fluidic channels

Isolating a single carbon nanotube and assembling it into an experimental platform may sound like a daunting task.

Hyegi Min, School of Energy and Chemical Engineering, Ulsan National Institute of Science and Technology, South Korea; hg1122@unist.ac.kr
Yun-Tae Kim, School of Life Sciences, Ulsan National Institute of Science and Technology, South Korea; kyt427@unist.ac.kr
Chang Young Lee, School of Energy and Chemical Engineering, Ulsan National Institute of Science and Technology, South Korea; cylee@unist.ac.kr
doi:10.1557/mrs.2017.57

© 2017 Materials Research Society
https://doi.org/10.1557/mrs.2017.57 Published online by Cambridge University Press

Luckily, a combination of electron microscopy, micro-/nanofabrication, and single-molecule spectroscopy enables not only fabrication of a single-CNT fluidic channel, but accurate control and measurement of the channel diameter, which has been challenging with other types of synthetic nanochannels. Here, we divide platforms into two categories—a supporting substrate upon which CNTs are deposited, and a membrane into which CNTs are embedded.

CNT channels on a substrate

The first platform type involves nanotubes directly synthesized on the substrate or deposited from a dispersion of nanotubes. The biggest advantage of this platform is its compatibility with conventional microfabrication and photolithography techniques, enabling researchers to control the number and the length of the nanotube channels, add markers for identification of specific channels, and pattern electrodes for monitoring and controlling the transport phenomena.

The process of forming a typical single-nanotube fluidic channel on a substrate was developed in 2010 by the Lindsay[5] and the Strano[8] groups. The Strano group's platform is illustrated in **Figure 1**a.[5,8,9] The process starts with the synthesis of horizontally aligned and millimeter-long single-walled carbon nanotubes (SWNTs) by chemical vapor deposition (CVD) involving the laminar flow of seeding gas.[13,14] After estimating the diameter and the chirality of CNTs with Raman spectroscopy, a single CNT with desired characteristics can be selected by removing all the others via plasma etching. A barrier structure having two compartments is then bonded onto the substrate.[5,8,9,15,16] Treating the entire structure with an oxygen plasma results in an open-ended CNT bridging the two compartments filled with electrolytes. Finally, the ion current through the interior of the CNT can be recorded while electrical bias is applied across the nanotube. Variations of this platform by the Lindsay group include patterning a gate electrode on the nanotube for controlling the transport,[4] adding microchannels for facile fluid exchange,[4,5] and using a transparent substrate for simultaneous electrical and optical recordings.[16]

CNT channels embedded into a membrane

A CNT can be embedded into a thin polymer membrane, a lipid bilayer, or membranes of a live cell. Although a soft membrane is not as mechanically robust as the platform previously described, this platform, when combined with microtomy, enables high-throughput fabrication of single-CNT channels all having the identical diameter and length. As the membrane is perpendicular to the molecular flux, molecules passing through the pore can be microscopically imaged by placing the membrane at the focal plane of the objective lens. In addition, a higher electric field across the short channel potentially allows transport of larger molecules.

Embedding a single CNT into a block of polymer, followed by slicing it into membranes, is a promising approach for making single-CNT fluidic channels with controlled diameter and length. This approach has been widely used in preparing multi-nanotube membranes,[11,17–19] however, the Crooks group is the only one that has taken this approach for a single-CNT study.[6,7,20,21] As depicted in Figure 1b, a forest of vertically aligned CNTs was synthesized by CVD. A single CNT pulled out from the forest is mounted onto a transmission electron microscope (TEM) grid and embedded into an epoxy matrix. After curing, the epoxy block is sliced using an ultramicrotome into many membranes containing identical CNT channels. The membrane is then placed between two chambers filled with electrolytes for recording the ion current. Although this platform may give reproducible data, as thousands of membranes can be generated from a single nanotube with controlled length, the method has been successful

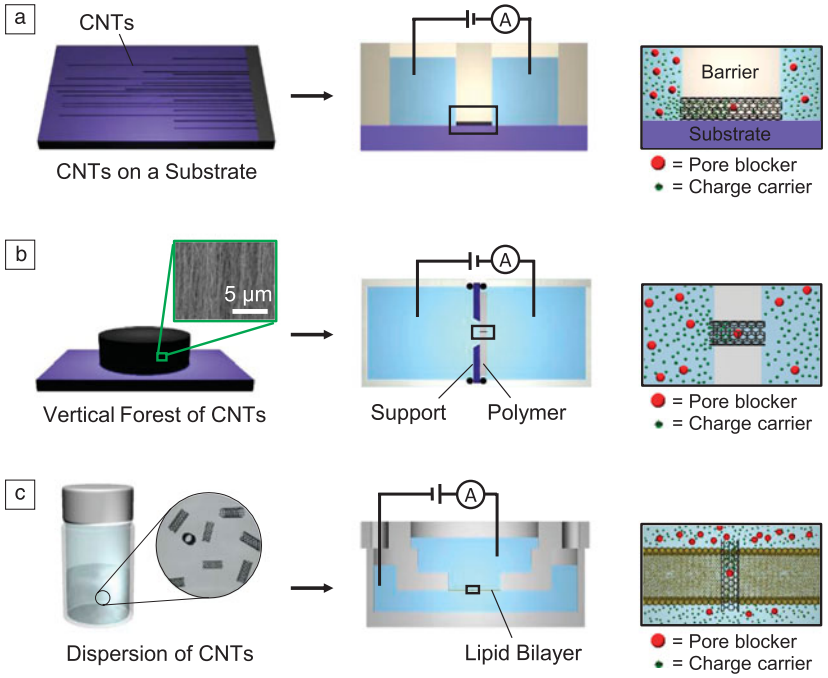


Figure 1. Various platforms for studying a single-carbon nanotube fluidic channel. (a) Carbon nanotube (CNT) channel on a substrate, covered by a barrier structure. Horizontally aligned and centimeter-long single-walled carbon nanotubes (SWNTs) are synthesized on a silicon wafer (left) to prepare a millimeter-long SWNT channel (center and right).[8] (b) CNT channel embedded in a polymer membrane. Vertically aligned forest of multiwalled carbon nanotubes (MWNTs) is synthesized on a silicon substrate (left), and a single-MWNT pulled out from the forest is embedded into a polymer membrane on a Si/Si_3N_4 support (center and right). Adapted with permission from Reference 7. © 2000 American Chemical Society. (c) CNT channel embedded into a lipid bilayer. Ultrashort (~10-nm-long) CNTs dispersed in an aqueous solution of surfactants (left) are inserted or self-assembled into a lipid bilayer (center and right). Adapted with permission from Reference 25. © 2014 Macmillan Publishers Ltd.

https://doi.org/10.1557/mrs.2017.57 Published online by Cambridge University Press

only with multiwalled carbon nanotubes (MWNTs, diameter >50 nm) and has yet to be tested with SWNTs.

Inserting a channel protein into a lipid bilayer is a well-established method in protein-ion channel research, and the nanotube research community has smartly adopted it by replacing the proteins with ultrashort CNTs (length <10 nm, Figure 1c). Wu's group inserted ultrashort CNTs into lipid bilayers using a syringe-connected micropipette.[22,23] A similar approach has been applied for inserting a CNT into a drilled solid-state membrane and sealing the gap by electron-beam-induced deposition of cracked naphthalene.[24] Noy and co-workers took the concept further and developed ultrashort CNTs that were capable of self-inserting into lipid bilayers, including living cell membranes, mimicking the behavior of biological pores such as α-hemolysin.[25] This feature allows bulk-scale measurements, for example, when applied to liposomes.[26] The platform also provides a stable baseline current and negligible background noise owing to the tight sealing around the CNTs.

Signals recorded from fluidic channels of CNTs

Molecular transport through a nanochannel is commonly detected by measuring ion current through the channel bridging two reservoirs of electrolytes. At a maximum sampling rate of 500 kHz (sampling every 2 μs) or higher, electrical recording is well suited for studying molecular events. The molecular behavior near the pore-mouth and within the CNT channel, however, cannot be fully understood by electrical measurements alone, and needs to be studied by additional approaches such as optical recordings.

Interpretation of the pore-blocking events

The current measured from an open channel is caused by stable flux of the charge carriers such as protons or ions of alkali metal halides. Often obscured by leakage current, the baseline current alone overestimates the flux through the CNT. Therefore, the role of blockers is crucial for unambiguously quantifying the flux of charge carriers through CNTs.

The ion-current trace provides ample information about the properties of the nanopore and the channel, charge carriers that contribute to the baseline current, and the blocker. A single blocker (red) enters an initially open CNT channel obstructing the otherwise stable flux of charge carriers (green), and leaves the channel from the other side restoring the flux (**Figure 2**a). A typical stochastic fluctuation of the ion current recorded from a single-CNT fluidic channel is shown in Figure 2b. The stochastic and two-state current trace is strong evidence of a single blocker transported through a single CNT. There are three important stages in the blocking event. Stage 1 (labeled "1" in Figure 2b) is the decrease in the ion current upon blockage, which corresponds to the amount of obstructed flux of the charge carriers by the blocker. The larger the blocker size, the greater is the magnitude of ion-current decrease. The maximum value of ion-current reduction in Stage 1, measured by varying the blocker size, therefore gives the unobstructed flux of the charge carriers. Stage 2 (labeled "2" in Figure 2b) is the duration of the blockage and represents the time it takes for the blocker to translocate to the other side of the CNT channel. When the tube length (L_{CNT}) and the electrical bias (V) are known, the velocity (v) and the mobility (μ) of the blocker can be calculated, respectively, as $v = L_{CNT}/2$ (where 2 in the denominator is the time interval labeled "2" in the figure) and $\mu = v/E$, where E denotes electric field ($= V/L_{CNT}$). Finally, Stage 3 (labeled "3" in Figure 2b) is called the open-channel lifetime, and represents how long the channel stays open until the next blocking occurs. This has often been overlooked in CNT channel studies, but it is important for understanding the kinetics of the blocker–CNT interaction. When the pore blockage is considered as a chemical reaction between the blocker and the CNT pore, the reaction-rate constant (k) can be extracted by analyzing the time interval of Stage 3.

Electrical detection of molecular transport

A single-CNT fluidic channel has enabled the study of individual nanoparticles, molecules, and ions. The long CNT channel, ranging from tens of nanometers to a few centimeters in length, extends the dwell time of the blocker, allowing for the study transport phenomena that is too fast to record in other types of nanopores. **Figure 3** shows blocking events caused by (a) polystyrene (PS) nanoparticles, (b) single-stranded DNA (ssDNA), and (c) hydrated cations. As expected, Figure 3a shows that large PS nanoparticles (d = 100 nm) block more current than smaller ones (d = 60 nm) when passing through a MWNT (d = 150 nm).[20] Such events can also be observed when a ssDNA blocks the ion current through an ultrashort SWNT (length ~10 nm) embedded in a lipid bilayer (Figure 3b, top).[25] Curiously, ssDNA passing through a 2-μm-long channel causes ion-current spiking (Figure 3b, bottom).[5,16,27] The current spiking is associated with a counterion layer around

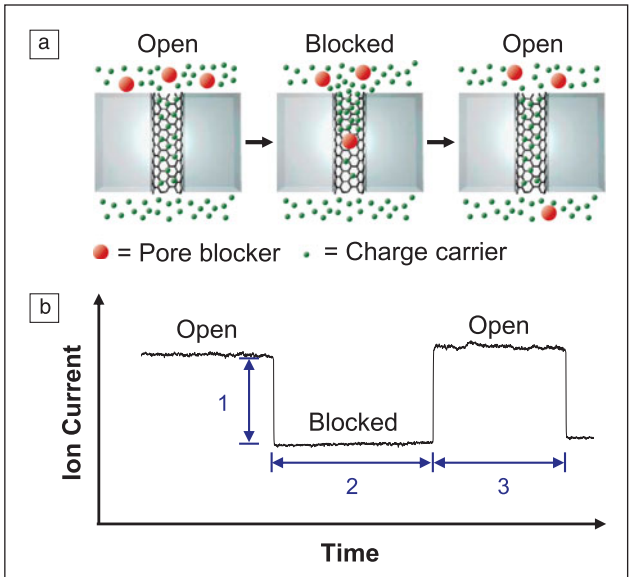


Figure 2. (a) Schematic of pore blocking events, and (b) stochastic fluctuation of the ion current depending on the position of the pore blocker.

https://doi.org/10.1557/mrs.2017.57 Published online by Cambridge University Press

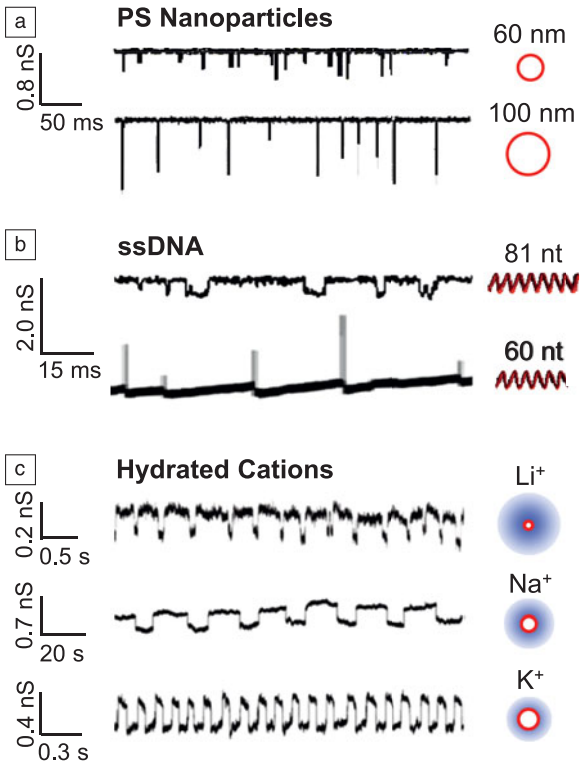


Figure 3. Electric detection of molecular translocation through a single-CNT channel with blockers for each trace depicted on the right. (a) Pore-blocking events caused by translocation of polystyrene (PS) nanoparticles with different sizes (60 nm and 100 nm). Adapted with permission from Reference 7. © 2000 American Chemical Society. (b) Blockage (top) and spiking (bottom) of the ion current caused by translocation of single-stranded DNA (ssDNA) through a single-walled carbon nanotube (SWNT). Adapted with permission from References 5 and 25. © 2010 AAAS and 2014 Macmillan Publishers Ltd., respectively. Here, "nt" stands for nucleotide and the zigzag symbol represents the helical structure of ssDNA. (c) Pore-blocking events caused by hydrated cations obstructing a proton flux through a SWNT. Red circles and shaded blue circles represent cations and hydration shells, respectively.[8]

DNA,[28] however, further studies are necessary to uncover the exact mechanism.

When the charge carriers and blockers are protons and hydrated cations, respectively, cations can be distinguished based on the obstructed proton flux (Figure 3c).[9] The proton flux through a 0.5-mm-long SWNT, ~10^8 protons/s, is comparable to the maximum value in biological proton channels (~10^9 protons/s), and the mobility of cations is orders of magnitude higher than the bulk mobility.[8] A unique feature of this long SWNT channel is the coherence resonance mechanism[29] in which the blocker-dependent oscillation of the ion current occurs spontaneously (Figure 3c). The oscillations occurring only in an optimal voltage range can potentially serve as a novel detection mechanism. The blocking events by cations are associated with the threshold voltage for shedding the hydration shells of the cations, as suggested by the diameter-dependent proton transport.[9] Guo et al.[30] provide a comprehensive review of single-CNT channels. Making a direct comparison between measurements in the literature is difficult due to the large variations in the experimental conditions. A standard protocol for testing the single-CNT fluidic channel will unambiguously examine the molecular transport.

Optical detection of molecular transport

The stochastic two-state current trace alone does not prove molecular transport through a single-CNT fluidic channel, so optical recordings of a single-CNT fluidic channel have been reported. Fluorescence images of a DNA translocating through a MWNT (**Figure 4**a)[6] appear promising, but such results using a SWNT have not yet been demonstrated. Lindsay's group simultaneously recorded optical and electrical signals when a fluorescence dye passed through a 20–30-μm-long SWNT.[16] They collected fluorescence from near the pore mouth, and spikes were detected in both the ion current and the fluorescence, with some delay caused by diffusion of dye molecules (Figure 4b). Each spike corresponds to transport of a single dye molecule.[16] Noy and co-workers performed a bulk-level optical measurement verifying fast proton transport along one-dimensional (1D) water wires formed in the confined interior of SWNTs. They inserted ultrashort SWNTs into a liposome (Figure 4c).[26] When the outer environment became more acidic than the interior, protons rushed into the liposome through the SWNT channels, causing the response from pH-sensitive fluorescence probe within the liposome. This ensemble measurement gave the per-nanotube proton conductance to be 2.5× greater than the proton conductance of a biological channel. This result suggests that CNTs can serve as efficient biomimetic nanopores.

Optical measurements in other nanofluidic channels provide insight into the study of single-CNT channels. Figure 4d shows optical detection of a DNA translocating through a protein-ion channel.[31] (i) When the pore is open, there is a flux of Ca^{2+}, and calcium-sensitive dyes fluoresce at the pore. (ii) When the pore is blocked by DNA, the fluorescence diminishes. (iii) DNA is released from the pore because of the negative potential, and fluorescence diminishes due to the reversal flux of Ca^{2+}. (iv) After applying 0 mV, fluorescence returns to its original state owing to Ca^{2+} flux. As this approach takes advantage of the large calcium flux through the protein channel, direct imaging of a single DNA is not necessary. Alternatively, direct imaging of a fluorescent labeled DNA is possible as the DNA translocates through a nanochannel (Figure 4e).[32] The entropic barrier was lowered by prestretching the DNA in an array of micropatterns. Future studies on a single-CNT fluidic channel should include these approaches if the platform can be fabricated reliably.

Summary and outlook

The unique 1D system with a tubular structure, as represented by CNTs, offers great promise in charge-specific transport, 1D chemical reactors, nanofluidic sensors, water purification, and desalination. CNT-based fluidic channels have several advantages over protein-ion channels, such as a smooth surface with controllable

https://doi.org/10.1557/mrs.2017.57 Published online by Cambridge University Press

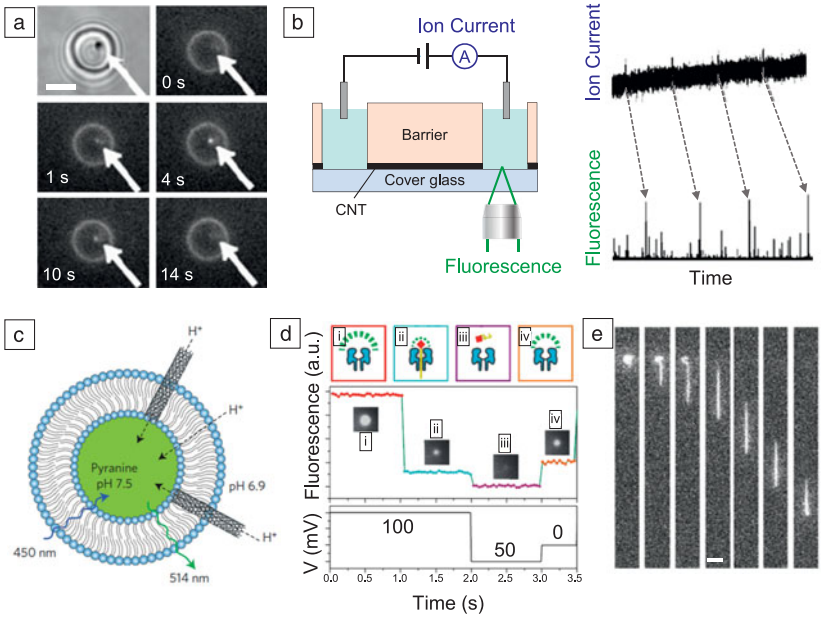


Figure 4. Optical detection of a single-molecule translocation through a nanochannel. (a) Series of images of DNA transported through a multiwalled carbon nanotube (MWNT) (77-nm dia. and 0.84-μm long). The top left is an optical image of the MWNT channel, and all the others are fluorescence images. As a DNA molecule approaches the focal plane near the carbon nanotube (CNT) pore, the fluorescence intensity spikes (4 s). The succeeding gradual decrease in intensity (10 s and 14 s) represents translocation of the molecule. Scale bar = 2.5 μm. Reprinted with permission from Reference 6. © 2003 Royal Society of Chemistry. (b) Experimental platform for optically detecting the translocation of a fluorescence dye through a single-walled carbon nanotube (SWNT) (left), and simultaneously recorded electrical and optical signal (right). Adapted with permission from Reference 4. © 2011 American Chemical Society. (c) SWNTs inserted into a liposome filled with proton-sensitive dyes and inward flux of protons through SWNTs when the exterior is more acidic than the interior of the liposome. Reprinted with permission from Reference 26. © 2016 Macmillan Publishers Ltd. (d) Fluorescence imaging of Ca^{2+} flux through a protein channel (α-hemolysin), which is blocked when the single-stranded DNA enters the pore. Reprinted with permission from Reference 31. © 2015 Macmillan Publishers Ltd. (e) Fluorescence images of a single λ-DNA flowing through a nanofluidic channel 160-nm wide, 220-nm deep, and 50-μm long. Scale bar = 5 μm. Reprinted with permission from Reference 32. © 2015 American Chemical Society.

geometry, chemical and physical robustness, and a wide range of available pore and sidewall chemistries. Therefore, applications demonstrated with a protein channel, such as single-molecule mass spectrometry,[33] characterization of peptides,[34] and DNA sequencing,[34–36] may be achieved more reliably with a CNT channel. A synergistic hybrid of CNTs and biological channels can be devised for improving the selectivity and reliability of existing systems. The biomimetic CNT channels embedded into both artificial and live-cell membranes suggest promising biological applications.

There are remaining challenges, however, because the recorded signals and their interpretations have been largely inconsistent across platforms. A large portion of the ambiguities can be resolved by implementing an imaging tool that visualizes what actually happens in the CNT channel. Real-time imaging of a single blocker and simultaneous recording of the ion current, for example, would give us confidence that the stochastic electrical signal originates from single-molecule events.

Acknowledgments

This work was supported by the Basic Science Research Program through the National Research Foundation of Korea (NRF) funded by the Ministry of Education, Science, and Technology (NRF-2013R1A1A2073264, NRF-2016R1C1B1013524) and the Nano Material Technology Development Program (2016M3A7B4910635). We also acknowledge valuable comments by A. Noy at the Lawrence Livermore National Laboratory.

References

1. J.K. Holt, *Adv. Mater.* **21**, 3542 (2009).
2. H.G. Park, Y. Jung, *Chem. Soc. Rev.* **43**, 565 (2014).
3. A. Noy, H.G. Park, F. Fornasiero, J.K. Holt, C.P. Grigoropoulos, O. Bakajin, *Nano Today* **2**, 22 (2007).
4. P. Pang, J. He, J.H. Park, P.S. Krstic, S. Lindsay, *ACS Nano* **5**, 7277 (2011).
5. H.T. Liu, J. He, J.Y. Tang, H. Liu, P. Pang, D. Cao, P. Krstic, S. Joseph, S. Lindsay, C. Nuckolls, *Science* **327**, 64 (2010).
6. T. Ito, L. Sun, R.M. Crooks, *Chem. Commun.* 13, 1482 (2003).
7. L. Sun, R.M. Crooks, *J. Am. Chem. Soc.* **122**, 12340 (2000).
8. C.Y. Lee, W. Choi, J.H. Han, M.S. Strano, *Science* **329**, 1320 (2010).
9. W. Choi, Z.W. Ulissi, S.F. Shimizu, D.O. Bellisario, M.D. Ellison, M.S. Strano, *Nat. Commun.* **4**, 2397 (2013).
10. R.B. Schoch, J.Y. Han, P. Renaud, *Rev. Mod. Phys.* **80**, 839 (2008).
11. J. Wu, K.S. Paudel, C. Strasinger, D. Hammell, A.L. Stinchcomb, B.J. Hinds, *Proc. Natl. Acad. Sci. U.S.A.* **107**, 11698 (2010).
12. X.L. Pan, Z.L. Fan, W. Chen, Y.J. Ding, H.Y. Luo, X.H. Bao, *Nat. Mater.* **6**, 507 (2007).
13. S.M. Huang, X.Y. Cai, J. Liu, *J. Am. Chem. Soc.* **125**, 5636 (2003).
14. Z. Jin, H.B. Chu, J.Y. Wang, J.X. Hong, W.C. Tan, Y. Li, *Nano Lett.* **7**, 2073 (2007).
15. W. Choi, C.Y. Lee, M.H. Ham, S. Shimizu, M.S. Strano, *J. Am. Chem. Soc.* **133**, 203 (2011).
16. W.S. Song, P. Pang, J. He, S. Lindsay, *ACS Nano* **7**, 689 (2013).
17. J. Wu, K. Gerstandt, M. Majumder, X. Zhan, B.J. Hinds, *Nanoscale* **3**, 3321 (2011).
18. J. Wu, K. Gerstandt, H.B. Zhang, J. Liu, B.J. Hinds, *Nat. Nanotechnol.* **7**, 133 (2012).
19. B. Lee, Y. Baek, M. Lee, D.H. Jeong, H.H. Lee, J. Yoon, Y.H. Kim, *Nat. Commun.* **6**, 7109 (2015).
20. T. Ito, L. Sun, R.M. Crooks, *Anal. Chem.* **75**, 2399 (2003).
21. T. Ito, L. Sun, R.R. Henriquez, R.M. Crooks, *Acc. Chem. Res.* **37**, 937 (2004).
22. L. Liu, J.I. Xie, T. Li, H.C. Wu, *Nat. Protoc.* **10**, 1670 (2015).
23. L. Liu, C. Yang, K. Zhao, J.Y. Li, H.C. Wu, *Nat. Commun.* **4**, 2989 (2013).
24. E. Secchi, A. Nigues, L. Jubin, A. Siria, L. Bocquet, *Phys. Rev. Lett.* **116**, 154501 (2016).
25. J. Geng, K. Kim, J.F. Zhang, A. Escalada, R. Tunuguntla, L.R. Comolli, F.I. Allen, A.V. Shnyrova, K.R. Cho, D. Munoz, Y.M. Wang, C.P. Grigoropoulos, C.M. Ajo-Franklin, V.A. Frolov, A. Noy, *Nature* **514**, 612 (2014).
26. R.H. Tunuguntla, F.I. Allen, K. Kim, A. Belliveau, A. Noy, *Nat. Nanotechnol.* **11**, 639 (2016).
27. J. He, H. Liu, P. Pang, D. Cao, S. Lindsay, *J. Phys. Condens. Matter* **22**, 454112 (2010).
28. J.H. Park, J. He, B. Gyarfas, S. Lindsay, P.S. Krstic, *Nanotechnology* **23**, 455107 (2012).
29. A.S. Pikovsky, J. Kurths, *Phys. Rev. Lett.* **78**, 775 (1997).
30. S.R. Guo, E.R. Meshot, T. Kuykendall, S. Cabrini, F. Fornasiero, *Adv. Mater.* **27**, 5726 (2015).
31. S. Huang, M. Romero-Ruiz, O.K. Castell, H. Bayley, M.I. Wallace, *Nat. Nanotechnol.* **10**, 986 (2015).
32. C. Wang, R.L. Bruce, E.A. Duch, J.V. Patel, J.T. Smith, Y. Astier, B.H. Wunsch, S. Meshram, A. Galan, C. Scerbo, M.A. Pereira, D.Q. Wang, E.G. Colgan, Q.H. Lin, G. Stolovitzky, *ACS Nano* **9**, 1206 (2015).

https://doi.org/10.1557/mrs.2017.57 Published online by Cambridge University Press

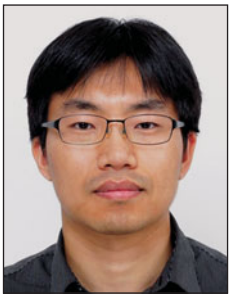
33. J.W.F. Robertson, C.G. Rodrigues, V.M. Stanford, K.A. Rubinson, O.V. Krasilnikov, J.J. Kasianowicz, *Proc. Natl. Acad. Sci. U.S.A.* **104**, 8207 (2007).
34. F. Bonardi, N. Nouwen, B.L. Feringa, A.J.M. Driessen, *Mol. Biosyst.* **8**, 709 (2012).
35. M. Fyta, *J. Phys. Condens. Matter* **27**, 273101 (2015).
36. I.M. Derrington, T.Z. Butler, M.D. Collins, E. Manrao, M. Pavlenok, M. Niederweis, J.H. Gundlach, *Proc. Natl. Acad. Sci. U.S.A.* **107**, 16060 (2010). □



Hyegi Min is a doctoral candidate in chemical engineering in the School of Energy and Chemical Engineering at Ulsan National Institute of Science and Technology (UNIST), South Korea. He received his BS degree in chemistry from UNIST. His research interests include molecular transport through the interior of single-walled carbon nanotubes and its chemical and biological applications. Min can be reached by phone at 82-52-217-2634 or by email at hg1122@unist.ac.kr.

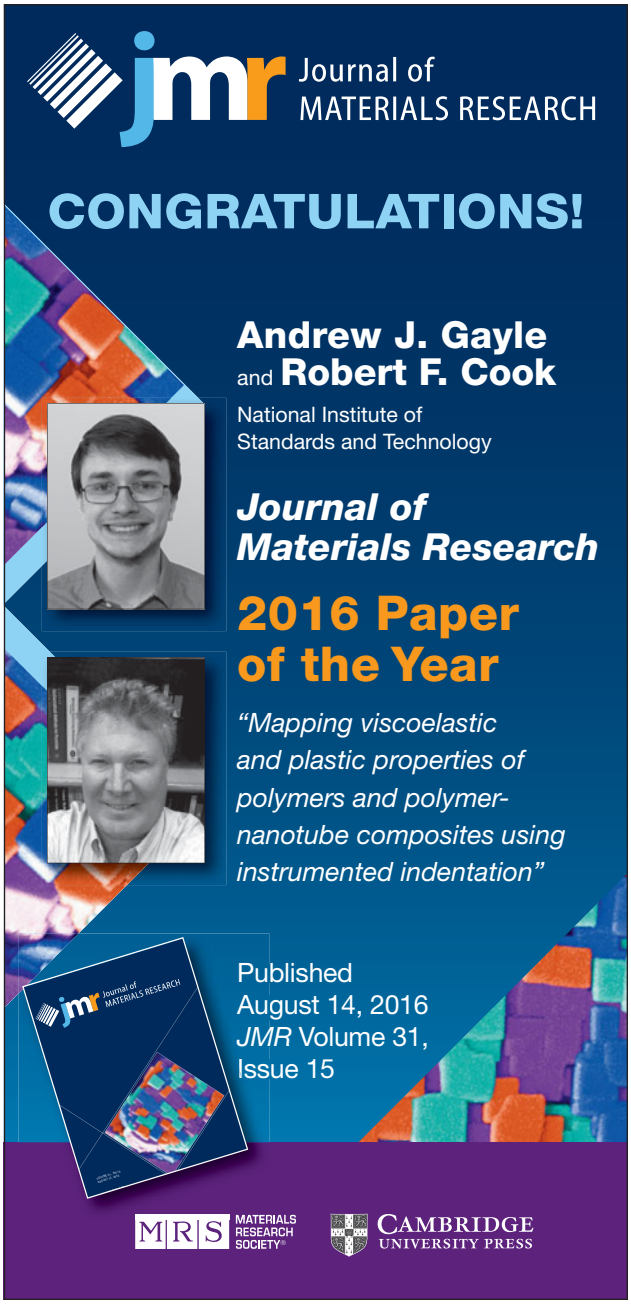


Yun-Tae Kim is a doctoral candidate in biomedical engineering at the Ulsan National Institute of Science and Technology, South Korea. He received his BS degree in biomedical engineering from the Catholic University of Daegu, South Korea, in 2013. His research focuses on the exterior transport of ions along carbon nanotubes and their applications in imaging and spectroscopy. Kim can be reached by phone at 82-52-217-2634 or by email at kyt427@unist.ac.kr.



Chang Young Lee is an assistant professor in the School of Energy and Chemical Engineering at Ulsan National Institute of Science and Technology (UNIST), South Korea. He received his BS degree from Seoul National University, South Korea, his MS degree from the University of Illinois at Urbana-Champaign, and his PhD degree in 2010 in chemical engineering from the Massachusetts Institute of Technology. Lee was a recipient of the 2009 Senturia Prize for Outstanding Thesis in Micro/Nanosystems from the Massachusetts Institute of Technology. His research interests include molecular transport in nanochannels and its applications in analytical chemistry. Lee can be reached by phone at +82-52-217-2547 or by email at cylee@unist.ac.kr.





https://doi.org/10.1557/mrs.2017.57 Published online by Cambridge University Press